NJC

PAPER

View Article Online
View Journal | View Issue

Cite this: *New J. Chem.*, 2017, **41**, 12319

Optical limiting properties of 3,5-diphenyldibenzo-azaBODIPY at 532 nm†

Gugu Kubheka, Ojodomo Achadu, John Mack * and Tebello Nyokong

Received 4th May 2017,
Accepted 21st September 2017

DOI: 10.1039/c7nj01503h

rsc.li/njc

Optical limiting properties of 3,5-diphenyldibenzo-azaBODIPY were investigated by using the z-scan technique at 532 nm in the nanosecond pulse range and a strong reverse saturable absorption (RSA) response was observed, which can be readily attributed to a two-photon absorption (TPA) assisted excited state absorption (ESA) mechanism in the singlet manifold based on a consideration of the other photophysical properties. The effect of solvent and incorporation into polymer thin films has been investigated in depth. The results indicate that the selection of solvents that enhance the population of the S_1 excited state on the nanosecond timescale or embedding the azaBODIPY dye into polymer thin films significantly improves the optical limiting properties.

Introduction

One of the main goals in the field of nonlinear optics has been the development of optical limiting (OL) materials. An ideal optical limiter must exhibit high transmittance of low-intensity light, but also be able to attenuate an intense optical beam, thus limiting the output fluence.[1–3] Consequently, considerable research has focused on creating ideal OL materials by exploiting different OL mechanisms including nonlinear scattering (NLS) and refraction (NLR), and nonlinear absorption (NLA) processes such as two-photon absorption (TPA), multi-photon absorption, reverse saturable absorption (RSA) and excited-state absorption (ESA).[4,5] The second harmonic of Nd/YAG laser systems at 532 nm has been the focus of considerable interest in this context in part due to concerns related to aviation safety and the irresponsible use of laser pens.[6–9] Numerous materials, including phthalocyanines,[10–12] porphyrins,[10,13] fullerenes,[1] carbon nanotubes,[14] nanoparticles,[15] metal nanowires,[16] and other organic chromophores[17,18] have been found to exhibit strong OL effects and have been explored as candidates for use in OL applications.

Boron dipyrromethene (BODIPY) dyes (Fig. 1) have been considered for a wide range of applications, due to their facile synthesis and structural modification, high molecular extinction coefficients and photostability.[19] They would not normally be considered for use in the context of the second harmonic of Nd/YAG lasers, however, since they typically absorb strongly in the green portion of the visible. Structural analogs of BODIPY dyes, such as azaBODIPYs (4,4-difluoro-4-bora-3*a*,4*a*-diaza-*s*-indacenes) have optical properties that are substantially modified and hence more suitable for OL applications at 532 nm (Fig. 1). AzaBODIPYs are formed by the substitution of the meso-carbon atom by an aza-nitrogen (Fig. 1B), which leads to a red-shift of the main absorption band of about 90 nm.[20] In the electronic absorption spectrum of 3,5-diphenyldibenzo-azaBODIPY (**1**) (Fig. 1), there is near zero absorbance in the 532 nm region, so there is little or no absorption of incident photons under normal light conditions.

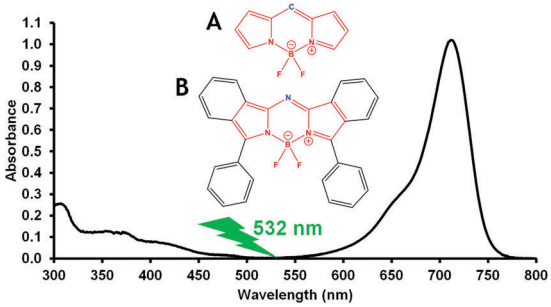

Fig. 1 The structures of the parent BODIPY dye (A) and 3,5-diphenyl-dibenzo-azaBODIPY (B) and the UV-visible absorption spectrum of **1** in DMSO.

The long π-conjugation system of the 3,5-diphenyldibenzo-azaBODIPY structure with two electron donating phenyl rings attached at either end and an electronegative aza-nitrogen atom at its core is somewhat analogous to the push–pull olefins that have been found to form unusually efficient two photon dyes.[21] Although the synthesis and characterization of 3,5-diaryldibenzo-azaBODIPY dyes have been undertaken by several researchers,[22,23] studies of these compounds are still somewhat limited because of their demanding synthesis and low yields.[23] There have been very few previous studies on the use of BODIPY dyes and their

Centre for Nanotechnology Innovation, Department of Chemistry, Rhodes University, Grahamstown 6140, South Africa. E-mail: j.mack@ru.ac.za

† Electronic supplementary information (ESI) available. See DOI: 10.1039/c7nj01503h

analogues as OL materials for 532 nm excitation pulses[24–26] and those at other wavelengths.[27–29]

From the point of view of OL applications, the nonlinear optical materials that are required for practical optical devices must meet the following four standards: (1) highly soluble compounds with weaker intermolecular interaction; (2) a high linear transmission; (3) a large nonlinear absorption with a sub-nanosecond response time over a broad spectral bandwidth; and (4) a high threshold for damage. Meeting all these criteria is still a significant challenge.[10] However, one of the strategies for the development of improved optical limiters is covalent or noncovalent combinations of NLO materials that have already been identified as good optical limiters.[30–34] Embedding optical limiting material in solid matrices is one practical strategy to improve the optical properties of these material. The use of poly(1,4-butylene carbonate) (PBC),[35] poly(methyl methacrylate) (PMMA)[36] and polystyrene (PS)[37] thin films as a strategy to improve optical limiting properties of optically active materials has been reported previously.

It has been demonstrated previously that the chemical environment influences the optical limiting efficiency of dyes that exhibit reverse saturable absorption,[38] so the chemical environment must be adjusted for any specific application to identify the conditions that provide the best possible optical response for an NLO material. This paper reports on the effects of matrix (*i.e.* in solution and solid state) on the OL (*i.e.* nonlinear absorption processes) of the 3,5-diphenyldibenzo-azaBODIPY. A comparison is made between the OL properties of aza-BODIPY **1** in a range of different solvents and when embedded into polymers as thin films in poly(1,4-butylene carbonate) (**1**_PBC), poly(methyl methacrylate) (**1**_PMMA) and polystyrene (**1**_PS). The concentration of the solutions was kept constant during the z-scan studies so that direct comparisons can be made.

Results and discussion

Spectroscopic characteristics

Fig. 2 shows the absorption spectra of **1** in different solvents such as dimethylsulfoxide (DMSO), EtOAc, tetrahydrofuran (THF), dichloromethane (DCM), toluene, benzene and CH_3CN at 1×10^{-5} M. As has been reported previously,[22] the absorption spectrum of **1** contains a characteristic intense visible region band that is associated with the HOMO → LUMO transition of the BODIPY chromophore. The marked red shift of this spectral band relative to that of BODIPYs is related to a stabilization of the LUMO due to there being a large MO coefficient on the electronegative nitrogen atom.[39] Since aza-BODIPYs are readily soluble in organic solvents,[22] linear Beer-Lambert plots are obtained for **1** in solution and this confirms the absence of significant aggregation at the concentrations used in this study. The spectrum measured in a PMMA thin film is almost identical to those obtained in organic solvents (Fig. 2). In contrast, there is a slight broadening and a small red shift of the main absorption band of **1** in PBC and PS (Fig. 2), but there is no evidence for a significant change

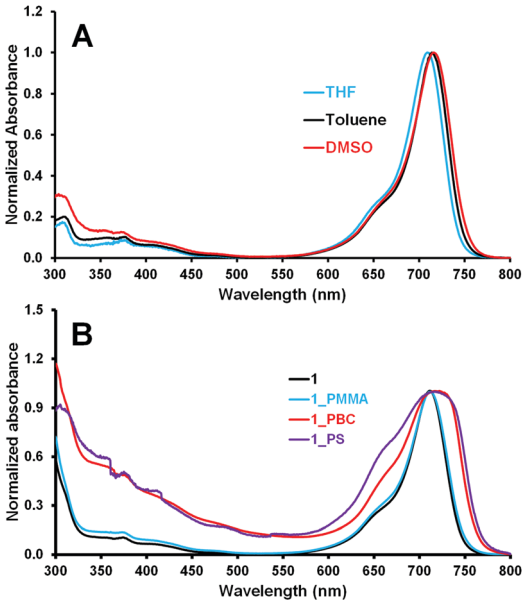

Fig. 2 Normalized UV-visible absorption spectra of **1** (A) in THF, toluene and DMSO and (B) in the **1**_PBC, **1**_PBC and **1**_PS thin films and the DCM solution used to prepare them. Details are provided in Table 1.

to the optical properties and electronic structure of **1** in this context. The increased absorbance in the 300–500 nm region can be attributed primarily to the polymer matrix.

Emission spectra of **1** are provided as ESI.† As would normally be anticipated, the emission bands are near mirror images of the $S_0 \rightarrow S_1$ absorption bands as would be anticipated for a complex with a rigid π-conjugation system. The shape of the fluorescence band is independent of the excitation wavelength indicating that the emission is from the lowest vibrational level of the S1 excited state,[40] because a very fast internal conversion process populates the fluorescent S_1 excited state. The fluorescence quantum yields (Φ_F) were determined using values that were reported previously for **1**,[41] by using a comparative method.[42] Fluorescence lifetime (τ_F) values were obtained by fitting fluorescence decay data and were found to decrease with increasing solvent polarity (Table 1). In contrast with classical BODIPY dyes that sometimes have Φ_F values as high as 1.0,[43] the Φ_F values of **1** are relatively low. No clear trends are observed in the Φ_F and τ_F values in terms of the polarity of the solvents (Table 1).

Table 1 Absorption and fluorescence properties of **1** in different solvents and in thin films

	Solvent	λ_{abs} (nm)	λ_{em} (nm)	Φ_F	τ_t (ns)
1	DMSO	716	741	0.06	1.62
1	THF	710	736	0.08	1.63
1	Toluene	714	740	0.10	1.97
1	DCM	710	733	0.14[a]	1.99
1	EtOAc	705	731	0.18	1.65
1	Benzene	715	738	0.15	2.07
1	CH_3CN	705	730	0.20[a]	1.60
1_PMMA	—	717	—	—	—
1_PBC	—	724	—	—	—
1_PS	—	724	—	—	—

[a] Φ_F values reported previously in ref. 22*c*.

Optical limiting properties

The open aperture z-scan technique was used to characterize the OL properties of the series of materials in the study.[44] OL can depend on NLA, NLS, or NLR. This study mainly focused on the NLA, where the material transmittance was measured by open aperture z-scan as a function of material position at 532 nm using *ca.* 10 ns pulses with varied input irradiances in a wide range of different solvents and polymer thin films.

NLO parameters

Open aperture z-scan measurements were performed according to the method described by Sheik-Bahae and co-workers[44–46] (eqn (1)–(3)),

$$T(z) = \frac{1}{\sqrt{\pi} q_0(z)} \int_{-\infty}^{\infty} \ln\left[1 + q_0(z) e^{-\tau^2}\right] d\tau \quad (1)$$

where

$$q_0(z) = \frac{\beta_{\text{eff}} I_{00} L_{\text{eff}}}{1 + z^2/z_0^2} \quad (2)$$

and

$$L_{\text{eff}} = (1 - e^{(-\alpha L)})/\alpha \quad (3)$$

and L and I_{00} are the pathlength and the on-focus peak input irradiance, respectively; α and β_{eff} are the linear and effective nonlinear absorption coefficients; and L_{eff}, z, and z_0 are the effective pathlength, the translation distance of the sample relative to the focal point of the z-scan instrumentation and the Rayleigh length, respectively. The Rayleigh length is defined as $\pi w_0^2/\lambda$, where w_0 is the beam waist at the focus ($z = 0$), which is defined as the distance from the beam centre to the point where the intensity reduces to $1/e^2$ of its on axis value, and λ is the wavelength of the laser beam.

A numerical form of eqn (1), is employed as a fit function to the experimental data.[44–46]

$$T(z) = 0.363e^{\left(\frac{-q_0(z)}{5.60}\right)} + 0.286e^{\left(\frac{-q_0(z)}{1.21}\right)} + 0.213e^{\left(\frac{-q_0(z)}{24.62}\right)} + 0.096e^{\left(\frac{-q_0(z)}{115.95}\right)} + 0.038e^{\left(\frac{-q_0(z)}{965.08}\right)} \quad (4)$$

The imaginary component of the third-order susceptibility ($\text{Im}[\chi^{(3)}]$) which depends on the speed of the NLA response and is related to the β_{eff} value through eqn (5):[47]

$$\text{Im}\left[\chi^{(3)}\right] = \frac{n^2 \varepsilon_0 c \lambda \beta_{\text{eff}}}{2\pi} \quad (5)$$

where ε_0, n and c are the permittivity of free space, the linear refractive index and the speed of light, respectively.

The second-order hyperpolarizability (γ) values of the materials, which is related to the interaction between the incident photons and the permanent dipole moment of the dyes, were calculated using eqn (6):[11,47]

$$\gamma = \frac{\text{Im}\left[\chi^{(3)}\right]}{f^4 C_{\text{mol}} N_{\text{A}}} \quad (6)$$

where N_{A} is the Avogadro constant, C_{mol} is the concentration of the active chromophore, and f is the Lorentz local field factor, which is defined as $f = \frac{(n^2 + 2)}{3}$.

The open aperture z-scans for **1** exhibit strong RSA responses in a wide range of solvents and polymer thin films.[48]

The effective nonlinear absorption coefficient (β_{eff}) values (Table 2) were obtained by fitting of the open aperture z-scan data using eqn (1)–(4) for a TPA-assisted ESA mechanism (Fig. 3 and 4). The RSA responses are characterized by a reduction in the transmission about the focus of the lens (Fig. 3 and 4), and are consistent with the positive effective nonlinear absorption coefficients. CH_3CN exhibits the largest RSA response followed by benzene, EtOAc, DCM, toluene, THF and then DMSO (Fig. 3) as would be anticipated based on the photophysical properties (Table 1). Solvents that enhance the Φ_{F} values do so because the population in the S_1 excited state on the nanosecond timescale is enhanced by a lower rate of non-radiative decay. Upon embedding **1** into polymer thin films, the open aperture z-scan exhibits a much stronger response than in the different solvents (Fig. 4), in the following order: PS > PBC > PMMA. The β_{eff} value is directly proportional to the magnitude of the RSA response of the open aperture z-scan curves, so the highest values of 89 and 160 esu were obtained in CH_3CN and polystyrene, respectively.

In addition to the other OL parameters that have been described, the limiting threshold (I_{lim}) (Table 2), the input fluence at which the transmittance is 50% of the linear transmittance value (Fig. 5), is an important measure of how suitable optical limiting materials are for applications, since low OL thresholds are essential. The International Commission

Table 2 Optical limiting properties of **1** in different solvents (1×10^{-5} M) and thin films obtained with 10 ns pulses at 532 nm wavelength

	Solvent	α (cm^{-1})	β_{eff} (esu)	K	I_{lim} (J cm^{-2})	$\text{Im}[\chi^{(3)}]$ (esu)	γ (esu)	I_{00} (MW cm^{-2})
1	DMSO	<0.01	15	$\approx 1 \times 10^6$	—	3.4×10^{-11}	7.8×10^{-31}	280
1	THF	<0.01	26	$\approx 4 \times 10^6$	—	5.5×10^{-11}	1.0×10^{-30}	280
1	Toluene	<0.01	28	$\approx 4 \times 10^6$	—	6.9×10^{-11}	1.0×10^{-30}	280
1	DCM	<0.01	30	$\approx 4 \times 10^6$	—	7.2×10^{-11}	1.1×10^{-30}	280
1	EtOAc	<0.01	40	$\approx 5 \times 10^6$	3.0	9.7×10^{-11}	1.4×10^{-30}	280
1	Benzene	<0.01	40	$\approx 6 \times 10^6$	2.8	9.7×10^{-11}	1.4×10^{-30}	280
1	CH_3CN	<0.01	70	$\approx 1 \times 10^7$	2.4	1.4×10^{-10}	3.4×10^{-30}	280
1_PMMA	—	10.7	75	$\approx 1 \times 10^4$	0.57	1.8×10^{-10}	3.4×10^{-30}	77
1_PBC	—	160	80	$\approx 3 \times 10^3$	0.48	2.2×10^{-10}	4.6×10^{-30}	95
1_PS	—	24.0	130	$\approx 5 \times 10^5$	0.33	2.4×10^{-9}	3.7×10^{-30}	145

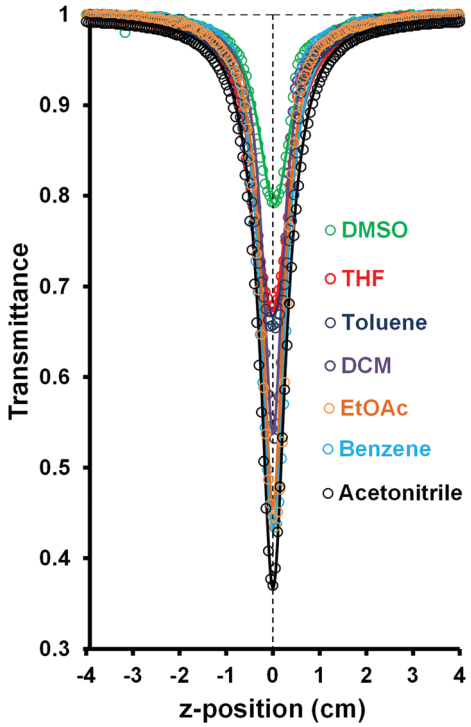

Fig. 3 Open-aperture z-scans showing the fitting for **1** in a wide range of different solvents. NLO parameters are provided in Table 2.

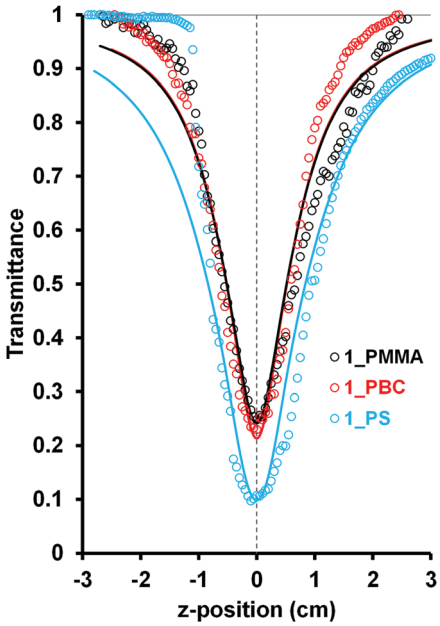

Fig. 4 Open-aperture z-scans for **1** in different polymer thin films. Detailed NLO parameters are provided in Table 2.

on Non-Ionizing Radiation Protection has published a guideline[49] for exposure limits to a variety of lasers. This study uses 10 ns pulses at 532 nm and, as such, the exposure limit can be determined from eqn (7),

$$2.7C_A t^{0.75}\ \text{J cm}^{-2} \quad (7)$$

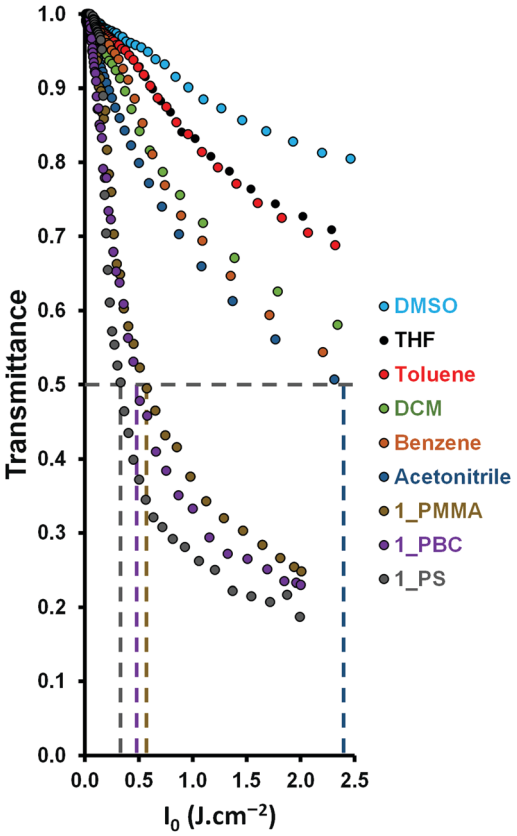

Fig. 5 Transmittance *versus* input fluence (I_0) curves for **1** in a series of different solvents and polymer thin films. The calculation for the I_{lim} values of **1** in PMMA, PBC, PS and CH_3CN are highlighted with dashed lines. Detailed NLO parameters are provided in Table 2.

where C_A is a correction factor (= 1 for 400–700 nm) and t is the exposure time. The exposure limit is 0.95 J cm^{-2} for a 0.25 s exposure time, since this is the average human blink reflex to a sudden flux of light.[50] The I_{lim} value can be derived by plotting transmittance against input fluence (Fig. 5). I_{lim} values of 3.0, 2.8 and 2.4 J cm^{-2} were determined for EtOAc, benzene and CH_3CN, respectively. The I_{lim} values for DMSO, THF, toluene and DCM could not be derived, since the transmittance did not reach as low as 50% of the linear transmittance at the input fluences that were used. I_{lim} values of 0.57, 0.48 and 0.33 J cm^{-2} were derived for **1**_PMMA, **1**_PBC and **1**_PS, respectively. This suggests that it should be possible to prepare polymer films that would form protective coatings on eyeware and on optical devices. The trend in the decrease in output fluence for all of the materials is consistent with the β_{eff} values (Table 2), since larger deviations from linear transmittance (Fig. 6) imply more effective optical limiting.

The OL properties have been interpreted on the basis of the absorption of 2 + 1 photons in the singlet manifold (Fig. 7), since in the absence of substitution with heavy atoms, BODIPYs and azaBODIPYs are known to have negligible triplet state quantum yields.[41,51] The K values provided in Table 2 are the excited state ratio and are defined as $K = \sigma_{ex}/\sigma_g$, where σ_{ex} and σ_g are excited state and absorption state cross-sections.

A large value of K is generally required to obtain a strong RSA response through an ESA mechanism.[52] Fitting of the open aperture z-scan data to eqn (4) yielded excited state cross-section (σ_{exc}) values for the materials that were in the 10^{-18}–10^{-15} range. Ground state absorption cross-sections (σ_{gr}) were estimated from eqn (8),[48]

$$\sigma_{gr} = \frac{\alpha}{N_0} \quad (8)$$

where α is the linear absorption coefficient and N_0 is the number of molecules per cm^3, and were found to be no higher than the 10^{-22} range, which is many orders of magnitude smaller than the σ_{exc} values as would be anticipated based on the very weak absorbance values in this spectral region (Fig. 1). Increased absorption in the excited states relative to the ground state is consistent with a mechanism in which ESA provides the observed RSA.

Further analyses for other OL parameters were carried out using methods described above,[11,47,53] Table 2. The estimated values for the imaginary component of the third order susceptibility ($Im[\chi^{(3)}]$) and second-order hyperpolarizability (γ) values are provided in Table 2. Both of these parameters need to be relatively large to facilitate a strong OL effect and low I_{lim} value.[44] The $Im[\chi^{(3)}]$ value is related to the speed of the OL response to intense incident laser light and should lie in the 10^{-9}–10^{-11} esu range with larger values being preferred,[47] since this implies the presence of a longer-lived virtual state that enhances the rate of TPA. The values both in solution and solid state lie within this range with significantly enhanced values obtained in the polymer thin films in the order of **1** < **1**_PMMA < **1**_PBC < **1**_PS (Table 2). The second-order hyperpolarizability values provide a useful parameter for comparing the relative efficiencies of OL materials based on the interaction between the incident photons and the permanent dipole moment of the dye molecule, lie in the 10^{-30}–10^{-31} esu range, which has previously been reported to provide an acceptable NLO response for use in OL applications.[54] The thin films have

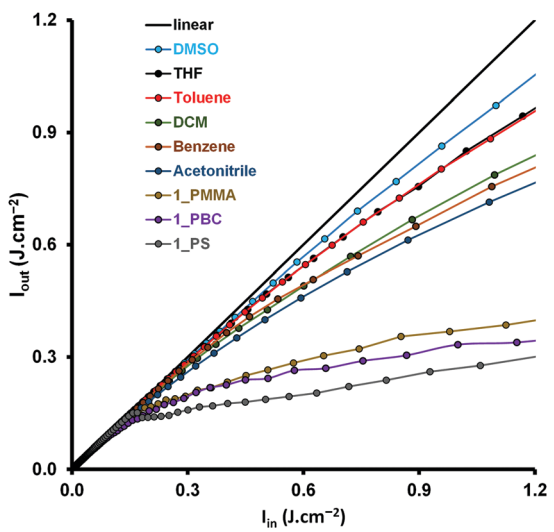

Fig. 6 Output fluence (I_{out}) *versus* input fluence (I_{in}) curves for **1** in a series of different solvents and polymer thin films. Detailed NLO parameters are provided in Table 2.

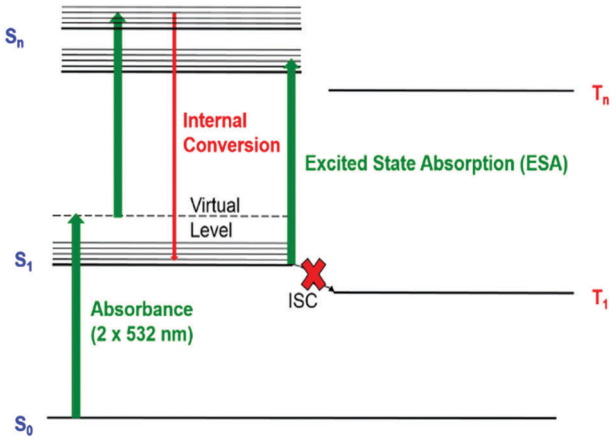

Fig. 7 Interpretation of the mechanism responsible for the observed RSA response.

significantly higher γ values than the solutions and hence provide significantly enhanced OL properties in this regard (Table 2). The trend in the γ values obtained in different solvents (Table 2) is similar to that observed in the Φ_F and τ_F values (Table 1), since the magnitude of both is related to the ability to populate the S_1 state of **1** on the nanosecond timescale.

Experimental

Materials

1 was synthesized according to the reported literature procedures.[22,41] Samples of spectroscopic grade DMF and DMSO were purchased from Sigma Aldrich and were used as received. Other solvents were dried and distilled prior to synthesis. All chemicals were analytically pure and were used as received for the synthesis of **1**.

Equipment

UV-visible absorption spectra were recorded on a Shimadzu UV-2550 spectrophotometer. Fluorescence spectra were measured on a Varian Eclipse spectrofluorimeter. Fluorescence lifetimes were measured using a time correlated single photon counting setup (FluoTime 200, Picoquant GmbH). The excitation source was a diode laser (LDH-P-670 driven by PDL 800-B, 670 nm, 20 MHz repetition rate, 44 ps pulse width, Picoquant GmbH). The z-scan experiments were performed using a frequency-doubled Quanta-Ray Nd:YAG laser as the excitation source. The laser was operated in a near Gaussian transverse mode at 532 nm (second harmonic), with a pulse repetition rate of 10 Hz and an energy range of 0.1 μJ–0.1 mJ limited by the energy detectors (Coherent J5-09). The low repetition rate of the laser prevents cumulative thermal nonlinearities. The beam was spatially filtered to remove higher order modes and tightly focused with a 15 cm focal length lens. A 2 mm quartz cuvette was used to obtain z-scan data in solution.

Synthesis of 1_PBC, 1_PMMA and 1_PS thin films

A drop and dry method was employed in the preparation of the polymer thin films. To 2.5 mL of **1** (1×10^{-5} M) solutions in

CH_2Cl_2, 100 mg of PBC, PMMA and PS were added to form the **1**_PBC, **1**_PMMA and **1**_PS thin films. The films were prepared by placing 200 μL of these solutions on a glass slide, which was left to dry in open air. Thin film thicknesses were determined to be 41, 29 and 49 μm by using the knife edge attachment of a Bruker D8 Discover X-ray diffraction (XRD) system.

Conclusions

The nanosecond timescale open aperture z-scan studies demonstrate that 3,5-diphenyldibenzo-azaBODIPY has significant OL properties at an excitation wavelength of 532 nm that are consistent with a TPA-assisted ESA mechanism and this results in a significant RSA response even in the absence of significant intersystem crossing to the triplet manifold. The trends observed in the magnitudes of the β_{eff} and γ values in a range of different solvents are similar to that observed in the Φ_F values, since in both cases the population of the S_1 state on a nanosecond timescale is the key factor. The OL properties are further enhanced in the context of the polymer thin films providing transmission values of less than 50% and I_{lim} values that are significantly below the threshold value that has been reported for damage to the human eye of 0.95 J cm^{-2}. Further studies are already in progress to investigate how the structural flexibility of BODIPY and aza-BODIPY dyes can be used to further enhance the OL properties.

Conflicts of interest

There are no conflicts of interest to declare.

Acknowledgements

This work was supported by the Department of Science and Technology (DST) and National Research Foundation (NRF) of South Africa through DST/NRF South African Research Chairs Initiative for Professor of Medicinal Chemistry and Nanotechnology, a CSUR grant from the NRF of South Africa to JM (uid: 93627), and a DAAD-NRF in-country doctoral scholarship to GK. Photophysical measurements were made possible by the Laser Rental Pool Programme of the Council for Scientific and Industrial Research (CSIR) of South Africa.

References

1 L. W. Tutt and A. Kost, *Nature*, 1992, **356**, 225–226.
2 J. W. Perry, K. Mansour, I. Y. S. Lee, X. L. Wu, P. V. Bedworth, C. T. Chen, D. Ng, S. R. Marder, P. Miles, T. Wada, M. Tian and H. Sasabe, *Science*, 1996, **273**, 1533–1536.
3 G. K. Lim, Z. L. Chen, J. Clark, R. G. S. Goh, W. H. Ng, H. W. Tan, R. H. Friend, P. K. H. Ho and L. L. Chua, *Nat. Photonics*, 2011, **5**, 554–560.
4 L. W. Tutt and T. F. Boggess, *Prog. Quantum Electron.*, 1993, **17**, 299–338.
5 J. Wang and W. J. Blau, *J. Opt. A: Pure Appl. Opt.*, 2009, **11**, 024001.
6 J. Shirk, R. G. S. Pong, F. J. Bartoli and A. W. Snow, *Appl. Phys. Lett.*, 1993, **63**, 1880–1882.
7 J. W. Perry, K. Mansour, S. R. Marder, K. J. Perry, D. Alvarez Jr. and I. Choong, *Opt. Lett.*, 1994, **19**, 625–627.
8 S. Hughes, G. Spruce, B. S. Wherrett and T. Kobayashi, *J. Appl. Phys.*, 1997, **81**, 5905–5912.
9 J. S. Shirk, R. G. S. Pong, S. R. Flom, H. Heckmann and M. Hanack, *J. Phys. Chem. A*, 2000, **104**, 1438–1449.
10 M. Calvete, G. Y. Yang and M. Hanack, *Synth. Met.*, 2004, **141**, 231–243.
11 Y. Chen, M. Hanack, Y. Araki and O. Ito, *Chem. Soc. Rev.*, 2005, **34**, 517–529.
12 Y. Chen, M. Hanack, W. J. Blau, D. Dini, Y. Liu, Y. Lin and J. Bai, *J. Mater. Sci.*, 2006, **41**, 2169–2185.
13 M. O. Senge, M. Fazekas, E. G. A. Notaras, W. J. Blau, M. Zawadzka, O. B. Locos and E. M. Ni Mhuircheartaigh, *Adv. Mater.*, 2007, **19**, 2737–2774.
14 P. Chen, X. Wu, X. Sun, J. Lin, W. Ji and K. L. Tan, *Phys. Rev. Lett.*, 1999, **82**, 2548–2551.
15 Y. P. Sun, J. E. Riggs, H. W. Rollins and R. Guduru, *J. Phys. Chem. B*, 1999, **103**, 77–82.
16 Y. P. Han, M. H. Luo, Q. W. Wang, J. X. Wang and X. L. Gao, *Adv. Mater. Res.*, 2011, **295**, 152–155.
17 Q. D. Zheng, S. K. Gupta, G. S. He, L. S. Tan and P. N. Prasad, *Adv. Funct. Mater.*, 2008, **18**, 2770–2779.
18 (*a*) Y. Li, B. O. Patrick and D. J. Dolphin, *Org. Chem*, 2009, **74**, 5237–5243; (*b*) A. B. Descalzo and K. Rurack, *Chem. – Eur. J.*, 2009, **15**, 3173–3185; (*c*) Y. Kubo, K. Yoshida, M. Adachi, S. Nakamura and S. Maeda, *J. Am. Chem. Soc.*, 1991, **113**, 2868–2873; (*d*) A. M. Barthram, R. L. Cleary, R. Kowallick and M. D. Ward, *Chem. Commun.*, 1998, 2695–2696; (*e*) H. Li, N. Nguyen, F. R. Fronczek and M. G. H. Vicente, *Tetrahedron*, 2009, **65**, 3357–3363.
19 Y. Kubo, K. Watanabe, R. Nishiyabu, R. Hata, A. Murakami, T. Shoda and H. Ota, *Org. Lett.*, 2011, **13**, 4574–4577.
20 T. H. Allik, R. E. Hermes, G. Sathyamoorthi and J. H. Boyer, *SPIE-Int. Soc. Opt. Eng.*, 1994, **2115**, 240–248.
21 T. Kogej, D. Beljonne, F. Meyers, J. W. Perry, S. R. Marder and J. L. Brédas, *Chem. Phys. Lett.*, 1998, **298**, 1–6.
22 (*a*) V. F. Donyagina, S. Shimizu, N. Kobayashi and E. A. Lukyanets, *Tetrahedron Lett.*, 2008, **49**, 6152–6154; (*b*) R. Gresser, M. Hummert, H. Hartmann, K. Leo and M. Riede, *Chem. – Eur. J.*, 2011, **17**, 2939–2947; (*c*) H. Lu, S. Shimizu, J. Mack, X.-Z. You, Z. Shen and N. Kobayashi, *Chem. – Asian J.*, 2011, **6**, 1026–1037.
23 (*a*) Y. Wu, D. H. Klaubert, H. C. Kang and Y.-Z. Zhang, *US Pat.*, 6005113, 1999; (*b*) J. H. Boyer and L. R. Morgan, *US Pat.*, 5189029, 1993; (*c*) G. Ulrich, S. Goeb, A. De Nicola, P. Retailleau and R. Ziessel, *Synlett*, 2007, 1517–1520; (*d*) L. Jiao, C. Yu, M. Liu, Y. Wu, K. Cong, T. Meng, Y. Wang and E. Hao, *J. Org. Chem.*, 2010, **75**, 6035–6038; (*e*) T. Okujima, Y. Tomimori, J. Nakamura, H. Yamada, H. Uno and N. Ono, *Tetrahedron*, 2010, **66**, 6895–6900.

24 M. Frenette, M. Hatamimoslehabadi, S. Bellinger-Buckley, S. Laoui, J. La, S. Bag, S. Mallidi, T. Hasan, B. Bouma, C. Yelleswarapu and J. Rochford, *J. Am. Chem. Soc.*, 2014, **136**, 15853–15856.
25 B. Kulyk, S. Taboukhat, H. Akdas-Kilig, J.-L. Fillaut, Y. Boughaleb and B. Sahraoui, *RSC Adv.*, 2016, **6**, 84854–84859.
26 M. Zhu, M. Yuan, X. Liu, C. Ouyang, H. Zheng, X. Yin, Z. Zuo, H. Liu and Y. Li, *J. Polym. Sci., Part A: Polym. Chem.*, 2008, **46**, 7401–7410.
27 B. Kulyk, S. Taboukhat, H. Akdas-Kilig, J.-L. Fillaut, M. Karpierz and B. Sahraoui, *Dyes Pigm.*, 2017, **137**, 507–511.
28 Q. Zheng, G. S. He and P. N. Prasad, *Chem. Phys. Lett.*, 2009, **475**, 250–255.
29 P. Bouit, K. Kamada, P. Feneyrou, G. Berginc, L. Toupet, O. Maury and C. Andraud, *Adv. Mater.*, 2009, **21**, 1151–1154.
30 Z. Liu, X.-L. Zhang, X.-Q. Yan, Y.-S. Chen and J.-G. Tian, *Chin. Sci. Bull.*, 2012, **57**, 2971–2982.
31 S. R. Mishra, H. S. Rawat, S. C. Mehendale, K. C. Rustagi, A. K. Sood, R. Bandyopadhyay, A. Govindaraj and C. N. R. Rao, *Chem. Phys. Lett.*, 2000, **317**, 510–514.
32 L. Vivien, P. Lançon, D. Riehl, F. Hache and E. Anglaret, *Carbon*, 2002, **40**, 1789–1797.
33 S. Wang, L. Zachary, S. C. Ivan and Q. Li, *RSC Adv.*, 2015, **5**, 41248–41254.
34 X. Zhang, Y. Feng, S. Tang and W. Feng, *Carbon*, 2010, **48**, 211–216.
35 C. Mkhize, J. Britton and T. Nyokong, *Polyhedron*, 2014, **81**, 607–613.
36 K. Sanusi and T. Nyokong, *J. Photochem. Photobiol., A*, 2015, **303–304**, 44–52.
37 N. Nwaji, J. Mack, J. Britton and T. Nyokong, *New J. Chem.*, 2017, **41**, 2020–2028.
38 M. Zawadzka, J. Wang, W. J. Blau and M. O. Senge, *Photochem. Photobiol. Sci.*, 2013, **12**, 1811–1823.
39 J. K. G. Karlsson and A. Harriman, *J. Phys. Chem. A*, 2016, **120**, 2537–2546.
40 F. L. Arbeloa, J. B. Prieto, V. M. Martínez, T. A. López and I. L. Arbeloa, *Int. Rev. Phys. Chem.*, 2005, **24**, 339–374.
41 P. Majumdar, J. Mack and T. Nyokong, *RSC Adv.*, 2015, **5**, 78253–78258.
42 (*a*) S. Frey-Forgues and D. J. Lavabre, *Chem. Ed.*, 1999, **76**, 1260–1264; (*b*) R. F. Kubin and A. N. Fletcher, *J. Lumin.*, 1982, **27**, 455–462.
43 A. Loudet and K. Burgess, *Chem. Rev.*, 2007, **107**, 4891–4932.
44 M. Sheik-Bahae, A. A. Said, T.-H. Wei, D. J. Hagan and E. W. Van Stryland, *IEEE J. Quantum Electron.*, 1990, **26**, 760–769.
45 M. Sheik-Bahae, A. A. Said and E. W. Van Stryland, *Opt. Lett.*, 1989, **14**, 955–957.
46 E. W. Van Stryland and M. Sheik-Bahae, in *Characterization Techniques and Tabulations for Organic Nonlinear Materials*, ed. M. G. Kuzyk and C. W. Dirk, Marcel Dekker, Inc., New York, 1998, pp. 655–692.
47 D. Dini and M. Hanack, in *The Porphyrin Handbook*, ed. K. M. Kadish, K. M. Smith and R. Guilard, Academic Press, USA, 2003, vol. 17, pp. 22–31.
48 R. L. Sutherland, *Handbook of Nonlinear Optics*, Marcel Dekker, New York, NY, 2nd edn, 2003.
49 R. Matthes, *Int. Comm. Health Phys.*, 2000, **79**, 431–440.
50 R. Hollins, *Curr. Opin. Solid State Mater. Sci.*, 1999, **4**, 189–196.
51 H. Lu, J. Mack, Y. Yang and Z. Shen, *Chem. Soc. Rev.*, 2014, **43**, 4778–4823.
52 P. de la Torre, F. Vázquez, T. Agulló-López and T. Torres, *J. Mater. Chem.*, 1998, **8**, 1671–1683.
53 B. E. A. Saleh and M. C. Teich, *Fundamentals of Photonics*, Wiley, New York, 1991.
54 X. Yan, T. Suzuki, Y. Kitahama, H. Sato, T. Itoh and Y. Ozaki, *Phys. Chem. Chem. Phys.*, 2013, **15**, 20618–20624.